Wearable Wireless Tyrosinase Bandage and Microneedle Sensors: Toward Melanoma Screening

*Bianca Ciui, Aida Martin, Rupesh K. Mishra, Barbara Brunetti, Tatsuo Nakagawa, Thomas J. Dawkins, Mengjia Lyu, Cecilia Cristea, Robert Sandulescu, and Joseph Wang**

Wearable bendable bandage-based sensor and a minimally invasive microneedle biosensor are described toward rapid screening of skin melanoma. These wearable electrochemical sensors are capable of detecting the presence of the tyrosinase (TYR) enzyme cancer biomarker in the presence of its catechol substrate, immobilized on the transducer surface. In the presence of the surface TYR biomarker, the immobilized catechol is rapidly converted to benzoquinone that is detected amperometrically, with a current signal proportional to the TYR level. The flexible epidermal bandage sensor relies on printing stress-enduring inks which display good resiliency against mechanical deformations, whereas the hollow microneedle device is filled with catechol-coated carbon paste for assessing tissue TYR levels. The bandage sensor can thus be used directly on the skin whereas microneedle device can reach melanoma tissues under the skin. Both wearable sensors are interfaced to an ultralight flexible electronic board, which transmits data wirelessly to a mobile device. The analytical performance of the resulting bandage and microneedle sensing systems are evaluated using TYR-containing agarose phantom gel and porcine skin. The new integrated conformal portable sensing platforms hold considerable promise for decentralized melanoma screening, and can be extended to the screening of other key biomarkers in skin moles.

1. Introduction

Wearable sensors have received considerable attention in recent years.[1,2] While most early studies have been devoted to the monitoring of vital signs and mobility, recent activity has been shifted to the noninvasive detection of chemical markers.[3–7] A variety of wearable optical and electrochemical sensors have thus been developed toward real-time analysis of body fluids, such as sweat or saliva, in connection to biomedical and fitness applications. Skin-worn and textile-based electrochemical sensors and biosensors have received particular attention toward epidermal monitoring of metabolites and electrolytes in connection to variety of flexible enzyme electrodes and ion-selective electrodes.[8–13] However, the ability to detect enzyme biomarkers has not been reported, nor have these wearable devices used for cancer screening applications.

We report here new fully integrated wearable bandage and microneedle electrochemical sensing platforms for detecting the enzyme tyrosinase (TYR) on both the skin surface and under the skin, respectively, toward potential melanoma screening. Since melanoma is an aggressive skin cancer, early diagnosis of the disease should lead to reduction in mortality. Currently, the identification of melanoma involves time-consuming complex techniques, aimed at detecting melanoma biomarkers, such as melanocytic lineage markers.[14,15] Due to the limitations of these methods, efforts have been devoted to faster and simpler detection of other melanoma biomarkers, such as the enzyme TYR. Tyrosinase is a polyphenol oxidase involved in the synthesis of melanin[14,16,17] whose overexpression and accumulation in skin cells can lead to the formation of skin melanoma.[18–20] TYR sensitivity approaches 100 percent for primary melanoma, with lower sensitivity in advanced stage of the disease. TYR screening is thus of considerable significance for practical clinical screening applications. Various laboratory-based methods, including electrochemical ones, have described for in vitro measurements of the TYR activity in skin tissues and biopsies.[21–24]

Wearable bandage-based electrochemical pH and uric acid sensors were developed recently for the monitoring of wound-healing processes.[25,26] The present bandage sensor (**Figure 1**D) incorporates a biocompatible hydrogel, containing the TYR substrate catechol (CAT). Since TYR is a polyphenol oxidase, it is capable of oxidizing *o*-diphenol substrates to the corresponding *o*-quinone compounds.[25,27] In the presence of the TYR, the immobilized catechol is oxidized to benzoquinone (BQ). The

B. Ciui, Dr. A. Martin, Dr. R. K. Mishra, Dr. B. Brunetti, Dr. T. Nakagawa, T. J. Dawkins, M. Lyu, Prof. J. Wang
Department of Nanoengineering
University of California
San Diego La Jolla, CA 92093, USA
E-mail: josephwang@ucsd.edu
B. Ciui, Prof. C. Cristea, Prof. R. Sandulescu
Analytical Chemistry Department
UMF
Cluj-Napoca 400349, Romania
Dr. B. Brunetti
DeFENS
University of Milan
Milan I-20133, Italy

DOI: 10.1002/adhm.201701264

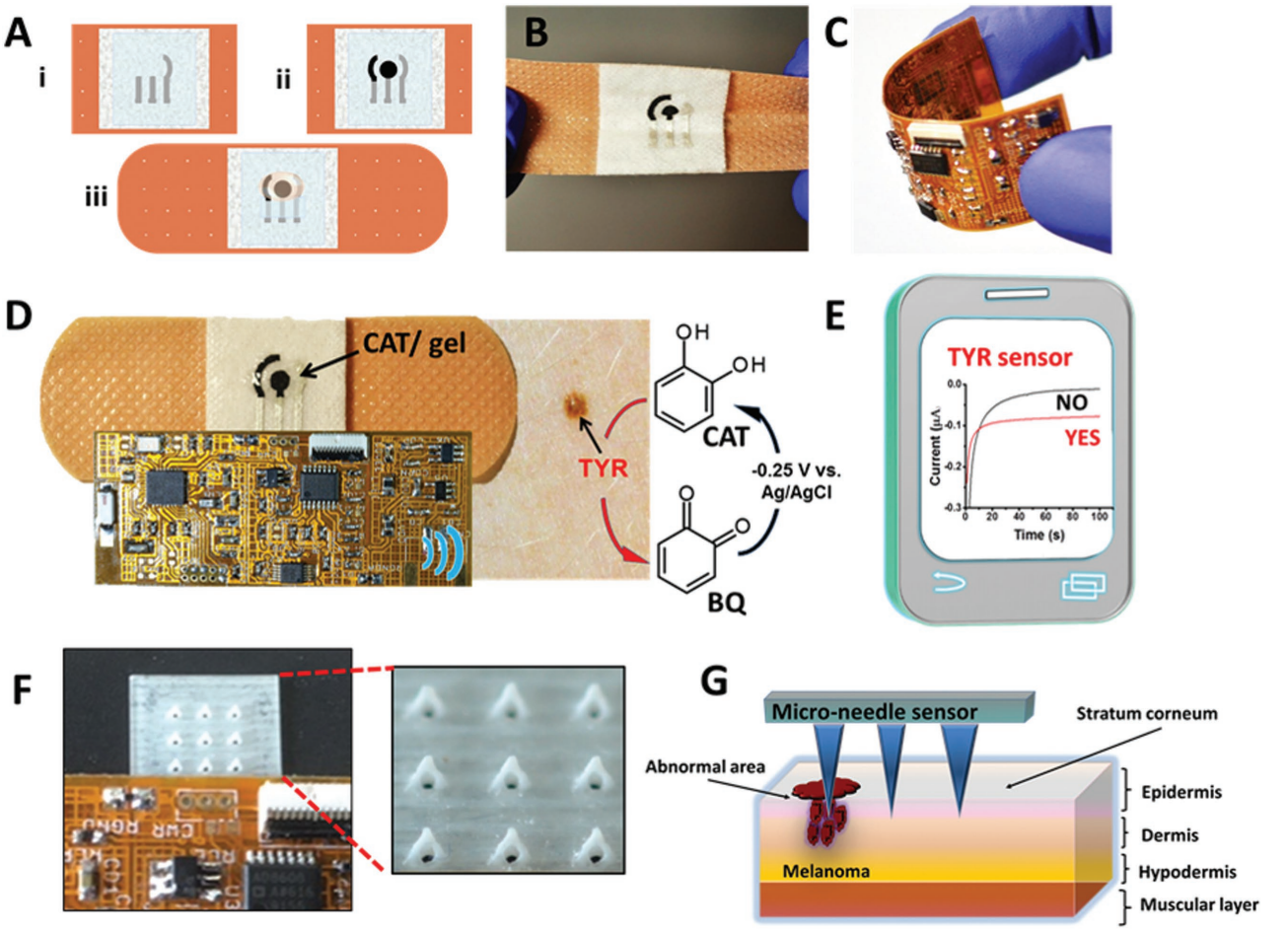

Figure 1. Bandage sensor for epidermal TYR monitoring toward melanoma screening: fabrication, features, and performance. A) Schematic of bandage sensor fabrication steps, (i) insulator, Ag/AgCl, (ii) carbon printing, and (iii) casting of agarose gel containing CAT. B) Image illustrating the bending of wearable bandage sensor and C) flexibility of the electronic board. D) TYR sensing procedure based on a bandage electrochemical sensor, combining a CAT-containing agarose gel, covering the three-electrode system, integrated to small flexible electronics. In presence of TYR, CAT is oxidized to BQ which is detected amperometrically by reduction at –0.25 V. The amperometric data is wirelessly transmitted E) to a smart device. F) Image of the microneedle sensor integrated to the soft flexible electronics. G) Schematic of the transdermal detection of TYR melanoma biomarker using the microneedle sensor.

BQ product is reduced and measured amperometrically at the printed carbon working electrode, at a potential of –0.25 V (vs Ag/AgCl). The three-electrode system on the bandage substrate is fabricated using stress-enduring compositions[28–30] in order to impart the flexibility during mechanical deformations (e.g., twisting and bending) expected during the placement and operation of the bandage (Figure 1B). The new skin-worn TYR bandage sensor has also been combined with a flexible electronic board that couples a miniaturized potentiostatic circuitry and wireless data transmission to perform such on-body amperometric detection of TYR. The polyimide-based bendable electronic board interfaces smoothly with the bandage TYR sensor, leading to a fully integrated, compact and conformal, easy-to-use, low cost, noninvasive melanoma screening system.

Along with the noninvasive bandage sensor, we describe also a minimally invasive microneedle sensing platform for TYR screening in transdermal tissues (Figure 1F). Such microneedle TYR sensor can physically pierce the upper layer of the skin, enhancing the access to deep skin tissue areas (Figure 1G). Minimally invasive electrochemical microneedle biosensors have been used for subcutaneous biosensing of glucose or lactate.[31,32] Microneedles have also been used recently toward the vaccination of melanoma,[33] and delivery of cosmetically relevant peptides.[34] Microneedle sensors (crossing of the top stratum corneum skin layer) can offer an attractive alternative route for reaching infected melanoma tissues and detecting the presence of TYR in these tissues. Microneedle biosensor arrays can thus potentially be used for skin cancer screening through the simultaneous monitoring of multiple disease biomarkers present in skin moles. Unlike early studies focusing on enzyme-based noninvasive monitoring of metabolites, the present work represents the first example of using wearable sensors for monitoring enzyme biomarkers. Overall, the new bandage and microneedle wearable sensors offer considerable promise for detecting TYR (and other skin cancer biomarkers), on both the skin surface and under the skin, respectively, toward rapid screening of melanoma. We envision that such wearable sensors could minimize the need of biopsies at

and doctors' offices and clinics, and related delays and anxiety, hence offering new possibilities of point-of-care cancer screening devices.

2. Results and Discussion

2.1. Dual TYR Bandage and Microneedle Sensors: Concept

The dual body-worn TYR sensors, described in this study, rely on noninvasive/minimally invasive amperometric detection of TYR on the skin surface and under the skin (transdermal tissues), respectively, toward rapid screening of melanoma. The TYR bandage sensor was fabricated by screen printing stress-enduring inks directly onto the soft fabric of a medical bandage toward future melanoma screening (Figure 1A). In the bandage sensor, the three-electrode system consisted of printing Ag/AgCl-Ecoflex mixed ink for the electronic contacts and reference electrode (i), along with carbon-based working and counter electrodes (ii). These two layers were printed on the top of a flexible insulator layer which improved the flexibility of the sensor performance and prevented permeation of the gel to the textile. The use of stress-enduring inks ensures the dynamic flexibility of the skin-mounted bandage (Figure 1B), without compromising the electrochemical performance. The bandage sensor is connected to a compact and flexible polyimide-based wireless electronic board (Figure 1C) that can operate under mechanical strain while conforming to the skin. This provides a skin-mounted fully integrated sensor platform. As shown in Figure 1D, followed by the modification with a catechol-containing agarose gel, the bandage sensor was directly attached onto the skin-mimicking phantom gel, covering the TYR-containing spots. The hydrophilic gel, containing the catechol, acts as a conducting layer completing the electrochemical cell, and allows a stable matrix for easy application onto the skin and optimal platform for the catechol to diffuse and interact with the surface TYR. The catechol substrate was selected owing to its favorable redox behavior on the carbon electrode. Thus, the TYR target is capable of oxidizing catechol (in-the-gel) to BQ, with the enzymatically generated quinone product measured amperometrically on the printed carbon transducer at –0.25 V. This bandage-based TYR sensor offers high selectivity, owing to the specific enzymatic reaction and low-potential detection of the product (see Section 2). The integrated TYR-bandage biosensor system thus combines the chemical-sensing capability with a wireless data transmission to a mobile device (Figure 1E) toward rapid on-body TYR detection and melanoma screening.

In addition to the bandage sensor, the microneedle sensor (Figure 1F) was also successfully integrated to the portable electronic board for TYR screening within the skin moles, following a similar amperometric detection protocol. The microneedle platform consisted of a 3×3 arrays of polymeric hollow microneedles (length of 800 μm), packed with catechol-coated carbon-paste (Figure 1F; see the Experimental Section for detail). The microneedle sensors were designed for penetration into skin tissues. Figure 1G depicts the concept of skin-piercing transdermal microneedle TYR sensor, penetrating a suspicious abnormal mole, while assuring a nearly painless sensing operation.

2.2. In Vitro Studies Using the TYR Bandage Sensor

The analytical performance of the bandage-based TYR sensor toward melanoma screening was tested by mimicking the human skin using a TYR-dosed agarose skin phantom. Phantom gels are commonly employed in diagnosis for in vitro research due to their skin-like properties and reproducible behavior.[35] Therefore, we designed a flexible 1×1 cm^2, 500 μm high PDMS platform to confine 1% w/v agarose-based skin phantom (**Figure 2**A). The phantom gel was spiked with different concentrations of TYR, ranging from 0.1 to 0.5 mg mL^{-1} that were allowed to diffuse into the gel before applying the bandage sensor. For each TYR screening test, a new skin phantom platform was used, because the immobilized catechol, reacting with the target TYR, is oxidized to BQ, as indicated by the brown color of the gel.

Figure 2B,C displays the amperometric response of the biosensor (interfaced with the flexible electronic board) to different TYR concentrations, ranging from 0.1 to 0.5 mg mL^{-1}. As expected, larger amounts of catechol were oxidized to BQ upon increasing the TYR level, resulting in a larger BQ reduction signal due to accumulation of the product in the agarose skin phantom. The low-cost bandage sensor is designed for single use; therefore, each experiment was performed using a new device, exhibiting a good reproducibility and performance. The TYR sensor responded with good linearity to increasing of TYR levels ($R^2 > 0.990$). Good sensitivity with linear dependence (slope of 4.6 ± 0.3 μA mg^{-1} mL^{-1} TYR) and a negligible intercept (0.07 ± 0.09 μA) are obtained. Further reproducibility tests were evaluated with triplicates of the calibration, showing good inter-bandage reproducibility with RSD <10% ($n = 3$), as illustrated in Figure 2C.

Since the TYR bandage sensor is aimed at a single-use testing of an abnormal mole, its long-term storage stability was evaluated. Long-term gel stability was studied to assess the performance of bandage sensor by applying 1×10^{-3} M catechol in 0.5 wt% agarose conductive gel over time. The bandage sensors were protected from sunlight and stored at room temperature and were subsequently electrochemically evaluated. For that, different cyclic voltammetric (Figure S1A, Supporting Information) and amperometric studies (Figure S1B, Supporting Information) were performed on the stored bandages for seven consecutive days. Both electrochemical techniques displayed a good performance of the bandage sensor containing the catechol gel over time. The voltammetric studies show very small change of the redox potential and current intensity, as illustrated in Figure S1A (Supporting Information); similarly, the amperometric data illustrated good interday stability, as shown in Figure S1B (Supporting Information). Such behavior of bandage sensor suggests good stability (RSD = 1.1%) of the bandage sensor over 7-day storage at room temperature, along with good sensor-to-sensor reproducibility.

Furthermore, different control experiments were performed including the absence of TYR (Figure 2D) and in the presence of TYR but without CAT (Figure 2E). The resulting data show no apparent change in the current response from the one obtained before interaction with the skin phantom gel, indicating the crucial role of the catechol substrate for the TYR analysis and the importance of polyphenols for the TYR activity.

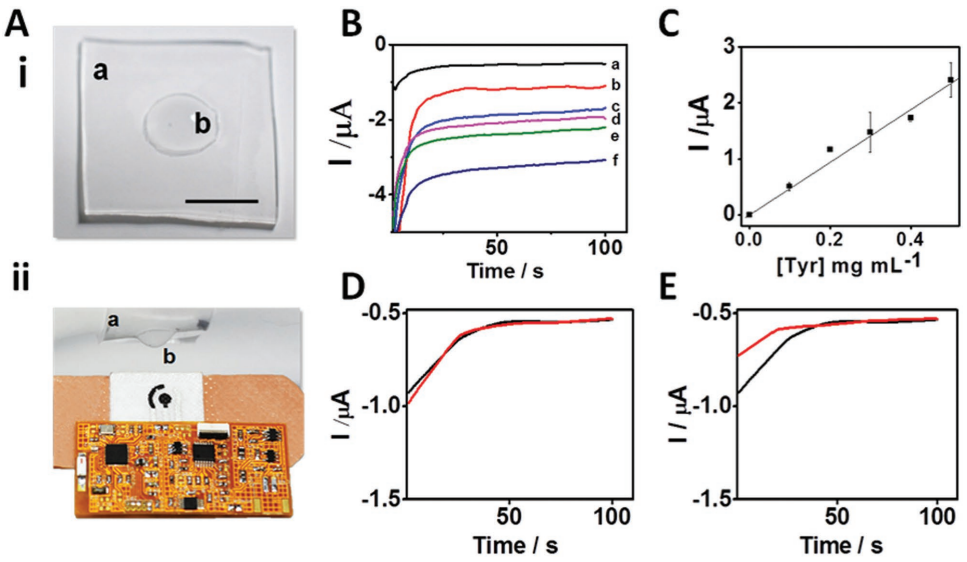

Figure 2. A) Images of (i) top and (ii) side views of flexible (a) PDMS layer imitating epidermal layer and (b) drop of phantom skin-gel containing TYR for in vitro TYR sensing; scale bar = 3 mm. B) Amperometric response of the bandage sensor using different TYR concentrations from 0 to 0.5 mg mL^{-1} (a–f) in the phantom gel (1% agarose). C) Corresponding current–TYR calibration plot. D) Amperometric response of bandage sensor before (black) and after (red) contact with TYR-free phantom gel, and E) in the absence of CAT, before (black) and after (red) the interaction with phantom gel containing 0.5 mg mL^{-1} TYR.

2.3. Selectivity of the Bandage Sensor

The bandage sensor offers high selectivity toward TYR screening because of the low negative potential used for the BQ detection and the low probability of catechol oxidation by other coexisting skin constituents. However, due to the potential presence of different electroactive skin constituents, the skin phantom gel was modified with common potential interferences, at their physiological concentrations, to evaluate their potential effect. **Figure 3**A displays the amperometric response recorded by the bandage sensor in the presence of 0.1 mg mL^{-1} TYR, showing distinct current signal of the target enzyme (red) relative to the background (black). In contrast, in the absence of TYR and the presence of other constituents of skin or sweat, such as ascorbic acid (Figure 3B), glucose (Figure 3C), uric acid (Figure 3D), histidine (Figure 3E), cysteamine (Figure 3F), and glutathione (Figure 3G), the amperometric response shows no distinguishable signal from that obtained before interaction with the "background" skin phantom gel. Other potential interferences, such as lactic acid, displayed negligible influence on the TYR signal (data not shown). Similar to glucose, lactic acid is not electroactive on the printed carbon electrode using

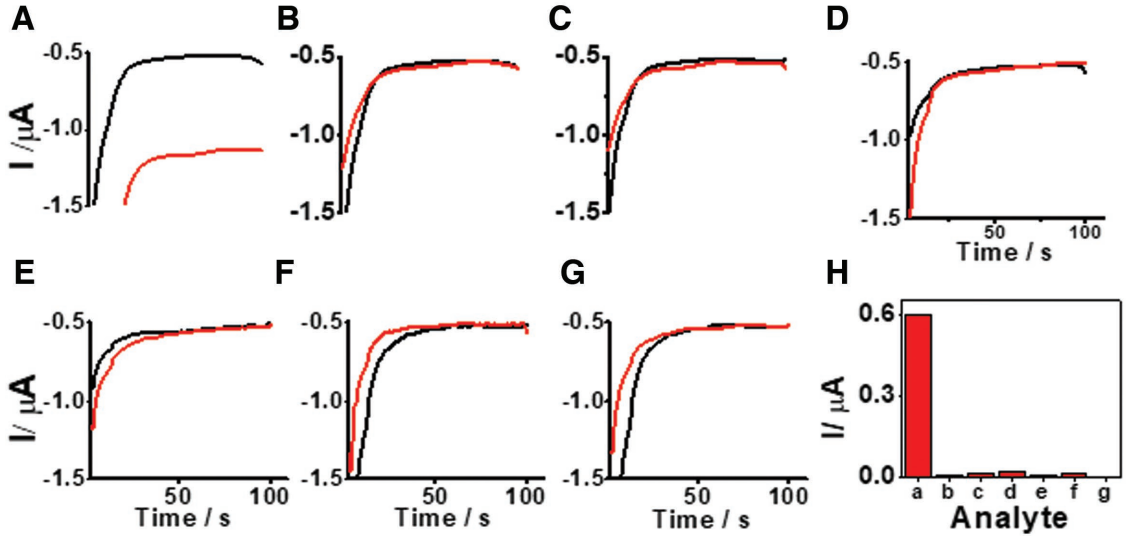

Figure 3. Sensor selectivity in the presence of potential interferences. Amperometric response of the bandage sensor before (black) and after (red) contact with phantom tissue containing, A) 0.1 mg mL^{-1} TYR, B) 1×10^{-3} M ascorbic acid, C) glucose, D) uric acid, E) histidine, F) cysteamine, and G) glutathione. H) Relative current values corresponding to different compounds in phantom tissue (A–G).

the operating detection potential. Such discrimination against common coexisting compounds reflects the high selectivity of the bandage sensor toward TYR screening.

2.4. Mechanical Resiliency of the TYR-Sensor

Bandage-based sensors are required to comply with the extreme mechanical strains associated with their placement on the human skin and sensing operation. To impart the high resilience against such deformations occurred on the bandage sensor, we relied on the stress-enduring inks for screen-printing.[28,29] To assess the impact of mechanical deformation/resilient on the response and overall analytical performance, the bandage sensor was exposed to multiple bends (**Figure 4**A) and twists (Figure 4B) while adhered onto skin and evaluated for its performance before and after the 100-iterative bending and twisting steps. Figure S2 (Supporting Information) illustrates the photographs before and after 100 successive twisting and bending deformation test. The bandage sensor appears to withstand multiple such mechanical deformations and maintain its attachment to the skin without compromising its electrochemical and conductive properties. The electrochemical properties of the printed bandage sensor were initially tested using 1×10^{-3} M catechol in the gel by CV measurements. Figure 4ii shows the effect on electrochemical performance after 100 repeated bending (Figure 4A) and twisting (Figure 4B) of the bandage sensor. Such repeated twisting and bending strains have a negligible effect on the electrochemical response of the bandage sensor, indicating resiliency against such multiple mechanical deformations. Subsequently, the bending studies were also performed in the presence and absence of conductive agarose gel on the bandage sensor surface. It was noticed that even after the 100-repeated bending in the presence of conductive agarose gel, the bandage sensor maintains a good sensing performance, indicating considerable promise for practical screening applications.

Dynamic resistance measurements were also carried out to assess the resiliency of the bandage sensor. Prolonged twisting and bending cycling were thus performed as shown in Figure 4iii and Video S1 (Supporting Information). The stress enduring electrodes were strained to a complete twisting and bending maneuvers (as shown in the Figure 4iii (a), and subsequent relaxation to initial position (as shown in Figure 4iii (b)). Upon repeated bend/relax cycling of the bandage sensor, the resistance between the carbon-based working electrode to the end of the silver contact pad was measured for bending and relaxing positions, using 30 s interval time between the relaxed (a) and stress (b) positions. These strains had a small effect on the electrode resistance, with an average resistance value of 270 ± 10 Ω and 90 ± 20 in relaxed position after twisting and bending, respectively. However, in the stressed positions, the resistance values increased to 500 ± 80 Ω and 380 ± 15 Ω during twisting and bending, respectively. Such small resistance changes after mechanical deformations indicate the potential applicability of the sensor under natural movement of the skin without compromising the electrochemical performance or electrical properties.

2.5. Microneedle Sensor for TYR Detection

The applicability of the catechol-containing microneedle sensor was evaluated by employing it onto the agarose phantom gel toward diverse level of TYR screening. First, the microneedle was used to evaluate the TYR reaction with catechol substrate and subsequently deployed for TYR screening in the skin phantom gel. A skin-mimicked phantom containing different

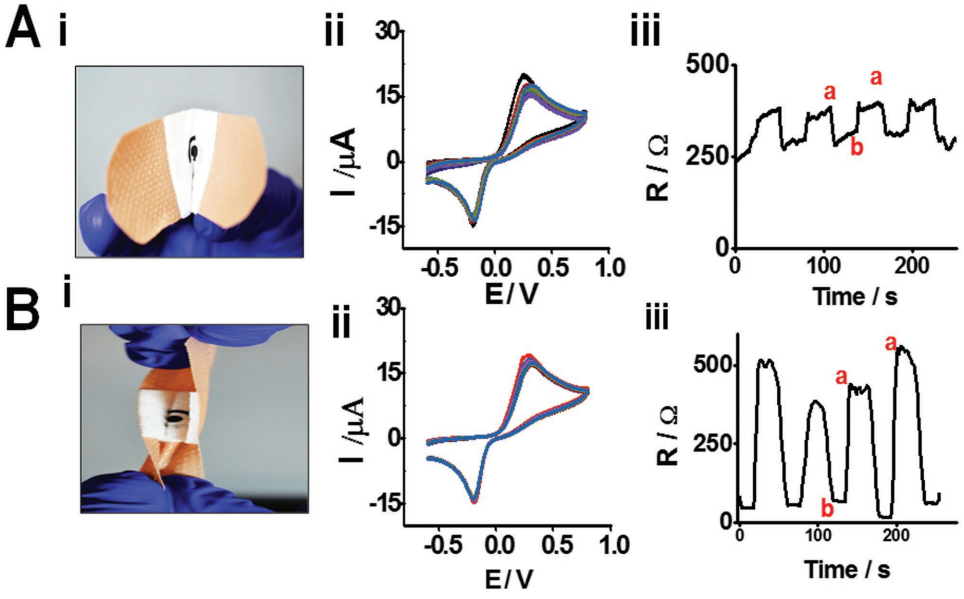

Figure 4. Dynamic mechanical deformations of the bandage sensor. Bending A) and twisting B) studies of the printed bandage sensor. (i) Images showing deformation of smart bandage sensor. (ii) Cyclic voltammetry of 1×10^{-3} M catechol (within 0.5% agarose gel) applying 100 iterative deformations, recorded after 20 such strains. (iii) Resistance measurements of the bandage, during (a) deformation and (b) relax cycles.

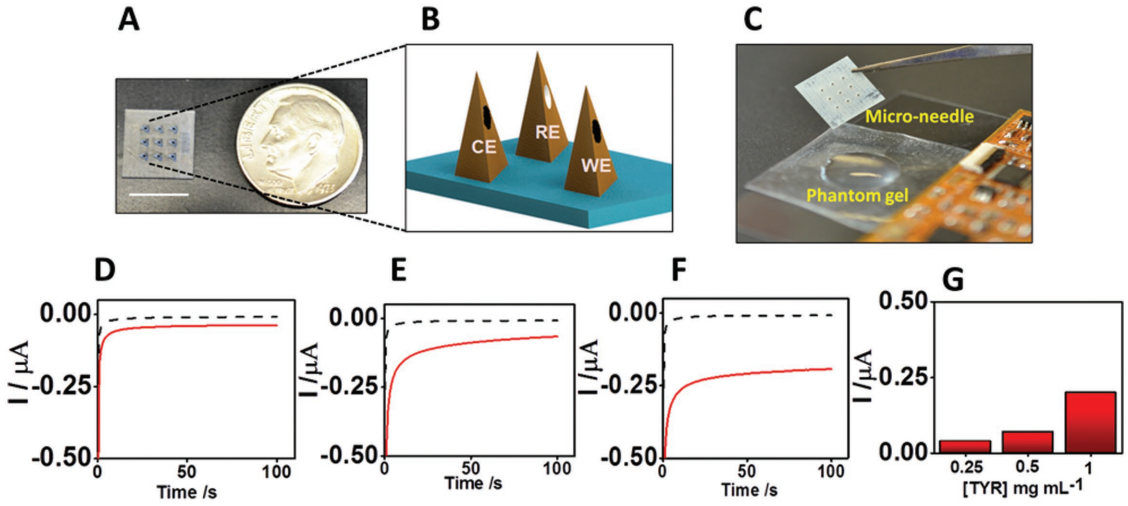

Figure 5. Feasibility of transdermal TYR screening in skin phantom gel using microneedle sensor. A) Actual image of carbon paste packed hollow microneedle in comparison with a penny; scale bar = 1 cm. B) Schematic of the pyramidal structure of the carbon filled microneedle's surface with WE, CE, and RE. C) Actual experimental setup mimicking skin phantom gel and microneedle used for TYR detection with integrated electronic board. Amperometric response of different TYR concentrations: D) 0.25, E) 0.5, and F) 1 mg mL^{-1}, before (black line) and after (red line) interaction with skin phantom gel; G) relative current values obtained from (D) to (F) amperograms.

TYR concentrations was used for assessing the performance of microneedle sensor and mimicking melanoma skin moles. The TYR diffusion on the phantom gel proceeded for 10 min, followed by piercing the microneedle sensor (loaded with catechol) and recording the amperograms after 2 min incubation. **Figure 5**A–C displays images of the carbon-paste packed arrays (3 × 3) of microneedles with actual size, shape, and distribution of WE, CE, and RE, and image showing the actual experimental setup with mimicked skin phantom gel and setting up the microneedle in order to detect the TYR dosing levels subsequently with wireless data transmission using integrated electronic board. Figure 5D–F shows the amperogram obtained with the microneedle sensor for transdermal detection of TYR in a phantom gel containing different TYR concentrations, whereas Figure 5G shows the relative current response of these varied TYR concentrations. It can be seen from Figure 5D–F that the carbon-packed microneedle sensor can readily detect different TYR levels within the skin phantom, compared to the control (TYR-free) phantom (dotted line). These current signals for the skin phantom increase proportionally upon increasing TYR level. The slightly lower current values, compared to the bandage sensor, reflect the smaller surface area of microneedle sensor (0.002 cm^2) versus bandage (0.07 cm^2). These results indicate the potential of the microneedle electrochemical sensor approach for on-body skin mole screening for possible melanoma screening in patients. Microneedle biosensor arrays could be used for the simultaneous monitoring of different analytes,[36] and could thus offer simultaneous detection of multiple biomarkers present in skin moles.

2.6. Ex Vivo Skin Model for TYR Screening

Porcine skin is structurally similar to the human epidermis, with similar thickness and dermal–epidermal thickness ratios. Thus, due to the similarity in TYR content of human tissues, porcine skin was selected to demonstrate measurements of the artificially dosed TYR content. Various experiments were thus carried out to demonstrate the potential of the developed bandage sensor toward TYR screening. Initially, porcine skin was dosed with different TYR levels and used to evaluate the potential of the bandage (**Figure 6**A) and microneedle (Figure 6B) sensors as potential melanoma screening tools. This demonstration involved dosing of a 1 × 1 cm^2 section of the pork skin with 0.5 mg mL^{-1} TYR (Figure 6Aii, Bii) and 2.5 mg mL^{-1} TYR (Figure 6Aiii, Biii). As shown in the insets of Figure 6, a change in skin color, from pink to dark brown, was observed after 24-h TYR diffusion due to the interaction of skin cells with TYR.[37] A clear darkening of the brown color is observed in Figure S3 (Supporting Information), from 0 to 24 h duration. The bandage (Figure 6A) and microneedle (Figure 6B) sensors were placed on the top of the spot generated by the TYR absorption. Subsequently, chronoamperometric measurements were performed on the untreated (Figure 6Ai and Figure 6Bi) and treated pork skin samples with 0.5 mg mL^{-1} (Figure 6Aii and Figure 6Bii), and 2.5 mg mL^{-1} TYR (Figure 6Aiii and Figure 6Biii), respectively. As illustrated in Figure 6, in the chronoamperometry plots no current response is observed using both the bandage (Figure 6A) and microneedle (Figure 6B) sensors for the TYR-free pork skin (i, red line), relative to the catechol background (i, black line). On the other hand, the TYR-treated skin samples display larger current signals upon increasing the TYR levels from 0.5 (Figure 6ii, red line) to 2.5 mg mL^{-1} (Figure 6iii, red line), relative to the catechol background (black line). Consequently, both the bandage and microneedle sensors were able to detect the presence of TYR on treated pork skin and discriminate between different levels of this enzyme biomarker in the skin tissues. This ex vivo study also signifies the total wearable integration of the bandage and microneedle sensors with the flexible wireless reusable electronic board toward for potential melanoma screening applications.

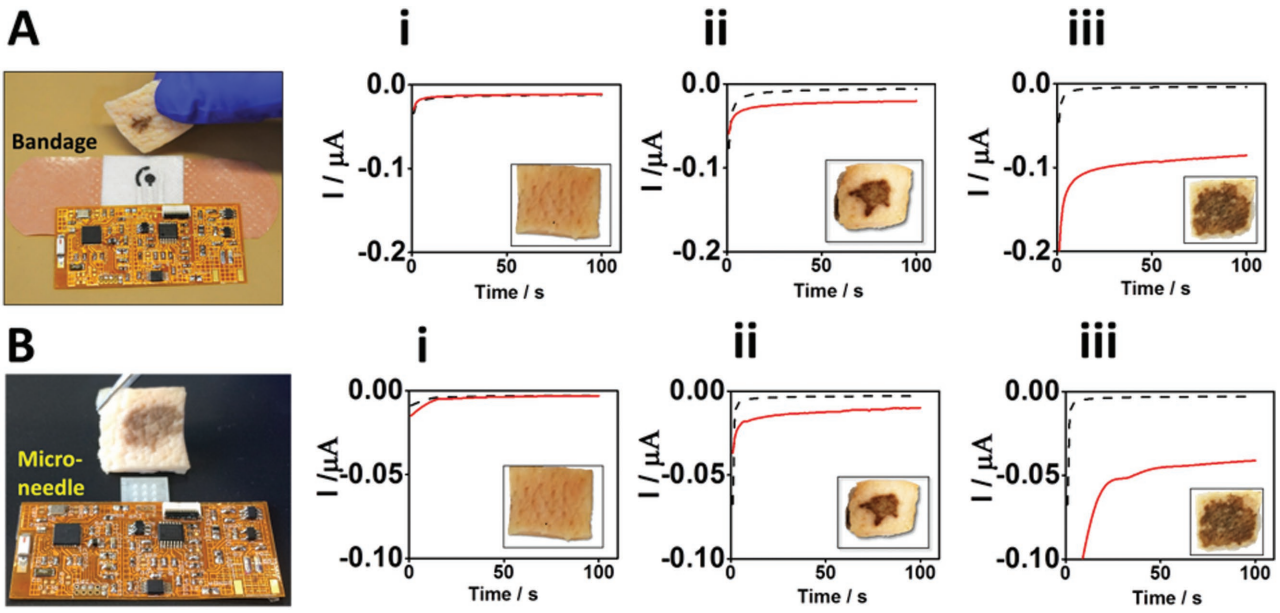

Figure 6. Ex vivo screening of Tyr in porcine skin model using the bandage A) and microneedle B) sensors. (Left) Images of fully integrated bandage (A) and microneedle (B) TYR-sensors on the treated pork skin. Amperometric response of the bandage (A) and microneedle (B) sensors before (black line) and after (red line) interaction with untreated pork samples (i), and samples treated with 0.5 mg mL^{-1} (ii), and 2.5 mg mL^{-1} TYR (iii). Insets show pictures of the untreated pork skin (i), and skin treated with 0.5 (ii) and 2.5 mg mL^{-1} (iii) TYR.

3. Conclusions

We have described new bandage and microneedle-based wearable TYR electrochemical sensors toward the decentralized screening of melanoma. To the best of our knowledge, this work represents the first wearable sensor for screening of TYR on skin and deep tissues toward future screening of melanoma tissues. The use of stress-enduring inks for printing the bandage sensor provides high resiliency against mechanical strains. The new skin-worn sensors have been interfaced with a conformal flexible electronic board that controls the electrochemical operation and wireless data transmission. Highly selective monitoring is achieved by immobilizing the CAT substrate of the TYR enzyme marker, and detecting the BQ reaction product amperometrically at a low-potential of −0.25 V. The resulting epidermal bandage and microneedle wearable sensors thus display an attractive analytical performance and offer considerable promise for detecting the TYR biomarker on both the skin surface and within skin moles, respectively, toward rapid screening of melanoma. In addition to clinical diagnosis, the new TYR wearable sensors offer considerable promise for assessing the quality of fruits and vegetables for the presence of pesticides, as shown in Figure S4 (Supporting Information). Future efforts will focus also on large scale clinical investigations aimed at measuring tyrosinase at the different stages of the cancer skin, along with a thorough validation, toward widespread melanoma screening. The new wearable devices are not limited to TYR screening, and can be extended toward the detection of other significant biomarkers in skin moles for wide range of skin cancer screening applications. Such epidermal skin cancer screening sensors could obviate the need of biopsy and associated delays and anxiety, and could eventually play a larger role, beyond skin cancer screening, toward cancer screening in general.

4. Experimental Section

Chemicals and Materials: All reagents and solvents were of analytical grade and used without further purification. Adhesive sterile bandages with nonadherent pad (2.5 × 7.6 cm; Honeywell Safety Products, Santa Ana, CA, USA), carbon ink (E3449, Ercon, Inc., Wareham, MA, USA), Ag/AgCl ink (E2414, Ercon, Inc., MA, USA), Ecoflex 00–30 (Smooth-On, Inc., Macungie, PA, USA), and permanent fabric adhesive (Aleene's, Inc., Fresno, CA, USA) were used. TYR from mushroom (lyophilized powder, 1000 unit mg^{-1} solid), CAT, disodium hydrogen phosphate, potassium dihydrogen phosphate, sodium chloride and potassium chloride, L-ascorbic acid, α-D-glucose, uric acid, L-histidine, cysteamine hydrochloride, L-glutathione oxidized disodium salt, and mineral oil (ρ = 0.838 g mL^{-1}) were purchased from Sigma-Aldrich (St. Louis, MO, USA). The graphite powder (crystalline 99%) was obtained from Alfa Aesar; Ward hill, MA) while agarose powder was purchased from MCB Manufacturing Chemists, Inc. (Gibbstown, NJ, USA).

Preparation of Stretchable Carbon and Ag/AgCl Inks and Electrode Fabrication: Stretchable inks were prepared as described in previous work.[29] Briefly, carbon ink was prepared by mixing 8.3 g Ercon carbon ink with 5% (1 g) polystyrene-block-polyisoprene-block-polystyrene (PS-PI-PS) prepared in 8 mL xylene. Afterward, mixture was placed in an ultrasound bath for 1 h, and homogenized in a shaker for 2 h. Ag/AgCl ink was prepared by mixing 9.5 g Ercon Ag/AgCl ink and 13 wt% of Ecoflex mixture (1:1 A and B of Ecoflex 00–30) using a Speed Mixer (DAC 150.1 FVZ, FlackTek Inc. (Landrum, SC) for 5 min at 2500 rpm. The electrode design was performed using AutoCAD (Autodesk, San Rafael, CA) and outsourced for fabrication on stainless steel through-hole 12″ × 12″ framed stencils of 125 μm thickness (Metal Etch Services, San Marcos, CA, USA). The printing process on the bandage consisted of first printing an insulating transparent adhesive layer comprised of flexible, stretchable adhesive ink (Aleene's Inc., Fresno, CA), followed

by Ag/AgCl and carbon layers, and finally, and an insulating layer (on top of the interconnects) to provide a dielectric separation of the three-electrode system and prevent device's short-circuits. Each printed layer was cured for 10 min at 75 °C.

Mechanical Resiliency Studies: The effect of mechanical stress on the printed bandages was analyzed by electrochemical measurements and dynamic resistance studies of the electrodes printed on the bandage. Bending experiments were carried out by completely bending to 180° and returning to a normal straight position, as shown in Video S1 (Supplementary Information) for 100 complete (straight-bend-straight) cycles. Twisting experiments were carried out by twisting in the middle part of the bandage and returning to a normal straight position. Cyclic voltammetry (CV) studies were carried out using 1×10^{-3} M catechol before and after 100 iterative twisting and bending steps. Resistance studies were carried out by dynamic testing using an Agilent 34411A digital multimeter (Agilent Technologies, Inc., Santa Clara, CA), sampling at a frequency of 1 Hz, and the Keysight BenchVue software (Keysight Technologies, Inc., Santa Rosa, CA) as a measuring interface.

Preparation of Hydrogel Bandage and Microneedle Sensors and Phantom Tissue Platform: A gel containing 1×10^{-3} M catechol and 0.5% agarose in 0.1 M phosphate buffer solution (PBS) (pH 7.4) was deposited on the three-electrode system. Initially, both powders were dissolved in the buffer. The resultant solution was stirred at 120 °C in an amber vial, to avoid photo-oxidation, until complete dissolution was obtained. Subsequently, 30 µL of the catechol-based gel solution was drop-casted on the electrode surface and allowed to cool down to room temperature. The sensor used 3 µg catechol per bandage. Considering this small amount and the short skin contact time (<2 min), the bandage sensor could be considered unharmful to the skin. In vitro and ex vivo studies were performed to comply the SOP approved by the institutional review board (IRB) of the University of California, San Diego, USA, which requires "no greater than minimal risk" to the prescreened subjects undertaken the investigation. Thus, for in vitro test, a standard phantom gel was used to simulate human tissue.[35] The tissue phantom gel was prepared by combining 0.1% w/v agarose powder with 0.1 M PBS (pH 7.4) while stirring in a glass vial at 170 °C. The TYR-containing gel was confined in a reservoir within a polydimethylsiloxane (PDMS) structure. Briefly, a 30:1 wt% mixture of PDMS-Sylgard Silicone Elastomer 184 and Sylgard Curing Agent 184 (Dow Corning Corp. Midland, MI) was spin coated at 250 rpm to get a 500 µm layer on silanized glass slides. The PDMS was cured at 80 °C for 60 min until the polymer was solidified and become rigid. Subsequently, 1 cm^2 square-shape pieces were cut and a 3 mm diameter × 500 µm depth hole was drilled before transferring the pieces to the mannequin surface for measurement with the bandage sensor. Warm agarose gel (7.5 µL) was poured into the hole of the PDMS structure and 2 µL of different concentrations of TYR in 0.1 M (pH 7.4) PBS were drop-casted and allowed to penetrate the phantom tissue for 10 min before measurement. During all measurements, the bandage sensor was placed on the target spot and allowed to react with the surface TYR for 2 min prior to the electrochemical measurement of the reaction product. The BQ product was measured amperometrically at the printed carbon working electrode using a potential of −0.25 V (vs Ag/AgCl).

Ex Vivo Screening of TYR in Pork Skin: Porcine skin was purchased from a local supermarket (San Diego, CA) and cut into 1 cm^2 area. Before use, the pork skin was sterilized using 70% ethanol to avoid any cross contamination and inhibition of the TYR activity. Then, 2 µL droplets containing different TYR concentrations were drop-casted onto the porcine skin and let it overnight in the refrigerator allowing diffusion into the skin. Following 24 h, the bandage-sensor and the microneedle sensor were applied on the affected area to test the presence of TYR.

Microneedle Device Fabrication: The hollow microneedle platform was fabricated similarly to earlier reports.[31,32] The microneedle array consisted in a 3 × 3 hollowed triangular base and pyramid-structured shape. The microneedle platform had an 800 µm height, and vertical circular openings of 425 µm diameter. The microneedle arrays were modeled through Solid works 3-D and printed by Perfactory SXGA Standard UV fast precursor system (EnvisionTEC GmbH, Gladbeck, Germany) through escorting light from a 150 W halogen bulb over a photocurable acrylate-polymer material (Eshell 200 Envision, TEC GmbH). After fabrication, the arrays were rinsed with isopropanol to clean the nonpolymerized substrate, and later were cured using a postcuring system (EnvisionTEC GmbH, Gladbeck, Germany).

Microneedle Packing: Sensor Fabrication: Three microneedles were chosen to perform the electrochemical sensing of TYR in skin moles from the 3 × 3 array of hollow microneedles. Carbon paste was packed on the chosen needles by mixing thoroughly graphite powder (65 wt %) and mineral oil (35 wt %) as binder until a homogeneous paste was formed. The carbon paste was filled in the three selected hollow microneedle pillars and the excess of paste was carefully removed from the pyramid surface. The resulting carbon paste surface was coated with the catechol-agar (phosphate-buffer) solution (see details below). The back of each packed microneedle was connected with wires using conductive silver epoxy to forge electrical contacts. Finally, the circular opening of hollow microneedles was polished using carbon paste for working and counter electrodes, whereas Ag/AgCl ink was used for reference electrode and was cured at 90 °C for 15 min.

Microneedle Sensor for TYR Screening: The microneedle was used to overcome the stratum corneum barrier and to detect TYR in transdermal tissues of skin moles. To do so, a skin phantom based on 1% agarose hydrogel was used to mimic the human skin, and the microneedle sensor was applied to detect different levels of spiked TYR in the phantom gel. In this study, 100 µL of phantom gel (prepared as previously described) was poured into the 10-mm diameter hole, opening in the PDMS substrate. Once the gel solidified, 2 µL droplets containing different TYR concentrations were dispensed on the skin phantom gel in order to mimic the melanoma cells containing TYR biomarker. Meanwhile, 0.5 µL of 1×10^{-3} M catechol, prepared in 0.5% agarose and 0.1 M PBS, was drop-casted onto the working area of the microneedle. Once the hydrogel was solidified, the microneedle was placed on the top of the skin phantom (piercing the hydrogel) and amperometric measurements were performed after 2 min incubation (to allow the TYR–catechol reaction) using an applied potential of −0.25 V over a 100 s period.

Electronic Board: The flexible printed circuit board (PCB) had been developed as the wireless electronic interface to support both bandage and microneedle amperometric operation. The bandage was integrated to the PCB by connecting the conductive wires from the PCB to the sensor using a copper tape. The carbon-paste packed microneedles were connected to the conductive wires on the PCB via stainless steel wires along with a conductive silver epoxy. The PCB contained a controller CC2640 from Texas Instrument (TI, Dallas, TX), which had an integrated Bluetooth Low Energy (BLE) function to enable wireless communication between the bandage-based melanoma screening sensor and a host device, such as smartphone or laptop. The fixed-potential between working and reference electrodes was generated by a digital-to-analog converter (DAC) from TI. A feedback loop compared the output of the DAC with buffered potential of the reference electrode, and controlled the potential of the counter electrode with a driver circuit. The DAC had 16-bits resolution and was controlled by the controller via serial peripheral interface. The output was sampled and digitized by an analog-to-digital converter (ADC) integrated in the controller. The sampling timing of the ADC, as well as the trigger for changing the output of the DAC, was controlled by a timer function in the controller. The current data from the sensor was once stored into the controller, and then transmitted to the host device as BLE packets. The data was displayed using a custom-made graphic interface in the host laptop. The flexible PCB was powered by a 3.6 V Li-ion rechargeable battery. The battery output was regulated using low dropout regulator (LP2981-33 from TI) to obtain 3.3-V precise and stable power for every circuit components. Also, an inverting DC–DC converter (LTC1983 from Linear Technology) was used to make nominal −3.6-V power source, which was supplied to the driver circuit of the counter electrode to extend the sweeping voltage range up to 1.2 V. All circuit components were implemented onto one side of a polyimide-substrate flexible board to conform to human body as a wearable sensor. The board size was as small as 50.8 × 24.1 mm.

Supporting Information

Supporting Information is available from the Wiley Online Library or from the author.

Acknowledgements

B.C., A.M, R.M., and B.B. contributed equally to this work. This work was supported by the Defense Threat Reduction Agency Joint Science and Technology Office for Chemical and Biological Defense (HDTRA 1-16-1-0013). B.C. acknowledges support of a Fulbright grant and UMF Cluj-Napoca, Romania (Grant no. 7690/24/15.04.2016).

Conflict of Interest

The authors declare no conflict of interest.

Keywords

amperometry, melanoma, microneedle sensor, tyrosinase screening, wearable flexible bandage sensors

Received: October 30, 2017
Revised: November 27, 2017
Published online:

[1] S. Nayak, N. R. Blumenfeld, T. Laksanasopin, S. K. Sia, *Anal. Chem.* **2017**, *89*, 102.
[2] A. J. Bandodkar, I. Jeerapan, J. Wang, *ACS Sens.* **2016**, *1*, 464.
[3] D. Diamond, S. Coyle, S. Scarmagnani, J. Hayes, *Chem. Rev.* **2008**, *108*, 652.
[4] W. Gao, S. Emaminejad, H. Y. Y. Nyein, S. Challa, K. Chen, A. Peck, H. M. Fahad, H. Ota, H. Shiraki, D. Kiriya, D-H Lien, G. A Brooks, R. W. Davis, A. Javey, *Nature* **2016**, *529*, 509.
[5] A. J. Bandodkar, J. Wang, *Trends Biotechnol.* **2014**, *32*, 363.
[6] M. D. Steinberg, P. Kassal, I. M. Steinberg, *Electroanalysis* **2016**, *28*, 1149.
[7] M. M. Rodgers, V. M. Pai, R. S. Conroy, *IEEE Sens. J.* **2015**, *15*, 3119.
[8] J. Kim, I. Jeerapan, S. Imani, T. N. Cho, A. Bandodkar, S. Cinti, P. P. Mercier, J. Wang, *ACS Sens.* **2016**, *1*, 1011.
[9] J. R. Windmiller, J. Wang, *Electroanalysis* **2013**, *25*, 29.
[10] M. Parrilla, R. Cánovas, I. Jeerapan, F. J. Andrade, J. Wang, *Adv. Healthcare Mater.* **2016**, *5*, 996.
[11] W. Jia, A. J. Bandodkar, G. Valdés-Ramírez, J. R. Windmiller, Z. Yang, J. Ramírez, G. Chan, J. Wang, *Anal. Chem.* **2013**, *85*, 6553.
[12] H. Y. Y. Nyein, W. Gao, Z. Shahpar, S. Emaminejad, S. Challa, K. Chen, H. M. Fahad, L. C. Tai, H. Ota, R. W. Davis, A. Javey, *ACS Nano* **2016**, *10*, 7216.
[13] H. Lee, T. K. Choi, Y. B. Lee, H. R. Cho, R. Ghaffari, L. Wang, H. J. Choi, T. D. Chung, N. Lu, T. Hyeon, S. H. Choi, D.-H. Kim, *Nat. Nanotechnol.* **2016**, *11*, 566.
[14] J. L. Boyle, H. M. Haupt, J. B. Stern, H. A. B. Multhaupt, *Arch. Pathol. Lab. Med.* **2002**, *126*, 816.
[15] D. Weinstein, J. Leininger, C. Hamby, B. Safai, *J clin. aesthet. dermatol.* **2012**, *7*, 13.
[16] J. Zhou, W. Shi, L. Li, Q. Gong, X. Wu, X. Li, H. Ma, *Anal. Chem.* **2016**, *88*, 4557.
[17] H. H. Hu, M. Guedj, V. Descamps, T. Jouary, A. Bourillon, K. Ezzedine, A. Taieb, M. Bagot, A. Bensussan, P. Saiag, B. Grandchamp, N. B. Seguin, N. Soufir, *J. Dermatol. Sci.* **2011**, *64*, 127.
[18] X. Yan, H. Li, W. Zheng, X. Su, *Anal. Chem.* **2015**, *87*, 8904.
[19] A. Ichikawa, H. Takagi, K. Suda, T. Yao, *Dermatology* **2009**, *219*, 195.
[20] A. R. Rao, H. N. Sindhuja, S. M. Dharmesh, K. U. Sankar, R. Sarada, G. A. Ravishankar, *J. Agric. Food Chem.* **2013**, *61*, 3842.
[21] R. Freeman, J. Elbaz, R. Gill, M. Zayats, I. Willner, *Chem. – Eur. J.* **2007**, *13*, 7288.
[22] H. B. Yildiz, R. Freeman, R. Gill, I. Willner, *Anal. Chem.* **2008**, *80*, 2811.
[23] M. Mossberg, S. Vernick, R. Ortenberg, G. Markel, Y. Shacham-Diamand, J. Rishpon, *Electroanalysis* **2014**, *26*, 1671.
[24] T. E. Lin, A. Bondarenko, A. Lesch, H. Pick, F. Cortes-Salazar, H. H. Girault, *Angew. Chem., Int. Ed.* **2016**, *55*, 3813.
[25] P. Kassal, J. Kim, R. Kumar, W. R. De Araujo, I. M. Steinberg, M. D. Steinberg, J. Wang, *Electrochem. Commun.* **2015**, *56*, 6.
[26] T. Guinovart, G. Valdés-Ramírez, J. R. Windmiller, F. J. Andrade, J. Wang, *Electroanalysis* **2014**, *26*, 1345.
[27] T. S. Chang, *Int. J. Mol. Sci.* **2009**, *10*, 2440.
[28] A. J. Bandodkar, I. Jeerapan, J. M. You, R. Nunez-Flores, J. Wang, *Nano Lett.* **2016**, *16*, 721.
[29] R. K. Mishra, L. J. Hubble, A. Martín, R. Kumar, A. Barfidokht, J. Kim, M. M. Musameh, I. L. Kyratzis, J. Wang, *ACS Sens.* **2017**, *2*, 553.
[30] Z. H. Jin, Y. L. Liu, J. J. Chen, S. L. Cai, J. Q. Xu, W. H. Huang, *Anal. Chem.* **2017**, *89*, 2032.
[31] G. Valdes-Ramirez, Y. C. Li, J. Kim, W. Jia, A. J. Bandodkar, R. Nunez-Flores, P. R. Miller, S. Y. Wu, R. Narayan, J. R. Windmiller, R. Polsky, J. Wang, *Electrochem. Commun.* **2014**, *47*, 58.
[32] J. R. Windmiller, N. Zhou, M.-C. Chuang, G. Valdés-Ramírez, P. Santhosh, P. R. Miller, R. Narayan, J. Wang, *Analyst* **2011**, *136*, 1846.
[33] Q. Zeng, J. M. Gammon, L. H. Tostanoski, Y.-C. Chiu, C. M. Jewell, *ACS Biomater. Sci. Eng.* **2017**, *3*, 195.
[34] Y. H. Mohammed, M. Yamada, L. L. Lin, J. E. Grice, M. S. Roberts, A. P. Raphael, H. A. E. Benson, T. W. Prow, *PLoS One* **2014**, *9*, e101956.
[35] A. Hellerbach, V. Schuster, A. Jansen, J. Sommer, *PLoS One* **2013**, *8*, e70343.
[36] P. R. Miller, S. A. Skoog, T. L. Edwards, D. M. Lopez, D. R. Wheeler, D. C. Arango, X. Xiao, S. M. Brozik, J. Wang, R. Polsky, R. J. Narayan, *Talanta* **2012**, *88*, 739.
[37] K. Iozumi, G. E. Hoganson, R. Pennella, M. A. Everett, B. B. Fuller, *J. Invest. Dermatol.* **1993**, *100*, 806.

